Structural Consequences of the B5 Histidine → Tyrosine Mutation in Human Insulin Characterized by X-ray Crystallography and Conformational Analysis[†,‡]

Lei Tang,[§,||] Jean L. Whittingham,*[,⊥] Chandra S. Verma,[⊥] Leo S. D. Caves,[⊥] and G. Guy Dodson[§,⊥]

Protein Structure Division, National Institute for Medical Research, The Ridgeway, London NW7 1AA, England, and Department of Chemistry, University of York, Heslington, York YO10 5DD, England

Received March 25, 1999; Revised Manuscript Received June 23, 1999

ABSTRACT: The addition of phenols to hexameric insulin solutions produces a particularly stable hexamer, resulting from a rearrangement in which residues B1−B8 change from an extended conformation (T-state) to form an α-helix (R-state). The R-state is, in part, stabilized by nonpolar interactions between the phenolic molecule and residue B5 His at the dimer−dimer interface. The B5 His → Tyr mutant human insulin was constructed to see if the tyrosine side chain would mimic the effect of phenol binding in the hexamer and induce the R-state. In partial support of this hypothesis, the molecule crystallized as a half-helical hexamer (T_3R_3) in conditions that conventionally promote the fully nonhelical (T_6) form. As expected, in the presence of phenol or resorcinol, the B5 Tyr hexamers adopt the fully helical (R_6) conformation. Molecular modeling calculations were performed to investigate the conformational preference of the T-state B5 Tyr side chain in the T_3R_3 form, this side chain being associated with structural perturbations of the A7−A10 loop in an adjacent hexamer. For an isolated dimer, several different orientations of the side chain were found, which were close in energy and readily interconvertible. In the crystal environment only one of these conformations remains low in energy; this conformation corresponds to that observed in the crystal structure. This suggests that packing constraints around residue B5 Tyr result in the observed structural rearrangements. Thus, rather than promoting the R-state in a manner analogous to phenol, the mutation appears to destabilize the T-state. These studies highlight the role of B5 His in determining hexamer conformation and in mediating crystal packing interactions, properties that are likely be important *in vivo*.

Insulin is a peptide hormone that interacts with specific cell surface receptors to stimulate glucose transport from the blood to muscle, adipose, and other tissues. It is used as an injected therapeutic agent for the treatment of diabetes mellitus. Owing to its crucial metabolic role and its pharmaceutical importance, many structural studies on chemically and genetically modified insulins have been carried out. These have produced a wealth of knowledge about the three-dimensional structure of insulin, resulting in significant improvements in insulin therapy (*1*−*4*). Insulin binds to its cell surface receptor as a monomer; however, during biosynthesis in the pancreas it forms hexamers by the association of three dimers around two zinc ions (Figure 1). The interactions made by the two central zinc ions are very specific, each one forming an octahedral coordination sphere with three B10 histidine side chains (one from each dimer) and three water molecules (*6*). The hexamer can be regarded as a dimer of trimers, one zinc ion associated with each trimer.

Owing to conformational variation at the beginning of the B chain, the insulin hexamer can adopt one of three distinct conformations, designated the T_6, T_3R_3, and R_6 states (Figure 1). In the T_6 insulin hexamer described above, residues B1−B8 of all six monomers are in an extended (T) conformation and are involved in close interdimer contacts (*6*). The six B5 His side chains in the hexamers occupy equivalent positions on the hexamer surface (Figure 1), such that B5 His of the first monomer in the dimer (known as molecule 1) makes a parallel ring-stacking interaction with the side chain of B5 His of molecule 2 in an adjacent hexamer. In the T_3R_3 hexamer, residues B1−B8 in molecule 2 of each dimer form an α-helix. This conformational rearrangement, which can be stabilized by the addition of sodium chloride (*7*, *8*), results in the displacement of residue B5 His of molecule 2 to a buried location at the dimer−dimer interface (Figure 1). Like the T_6 hexamer, the T_3R_3 hexamer contains at least two coordinated zinc ions. Owing to the packing of the B-chain N-terminal α-helices, the zinc ion at the center of the R_3 trimer occupies a more restricted space than that in the T_3 trimer and has a smaller, tetrahedral coordination sphere consisting of three B10 histidine side-chain ligands and a chloride ion. It has been shown that residue B5 His of

[†] This work was supported in part by the BBSRC.

[‡] The coordinates for the three B5 Tyr mutant insulin structures have been deposited in the Protein Data Bank at the EBI Macromolecular Structure Database, EMBL outstation Hinxton, European Bioinformatics Institute, Wellcome Trust Genome Campus, Hinxton, Cambridge CB10 1SD, U.K. The coordinate ID codes are 1QJ0 (ligand-free), 1QIY (with phenol), and 1QIZ (with resorcinol).

* To whom correspondence should be addressed. Email: jean@yorvic.york.ac.uk. Tel: +44-1904-432589. Fax: +44-1904-410519.

[§] National Institute for Medical Research.

[||] Present address: Laboratory of X-ray Crystallography, Dana-Farber Cancer Institute, Smith Building, 1 Jimmyfund Way, Boston, MA 02115.

[⊥] University of York.

10.1021/bi990700k CCC: $18.00
Published on Web 08/21/1999

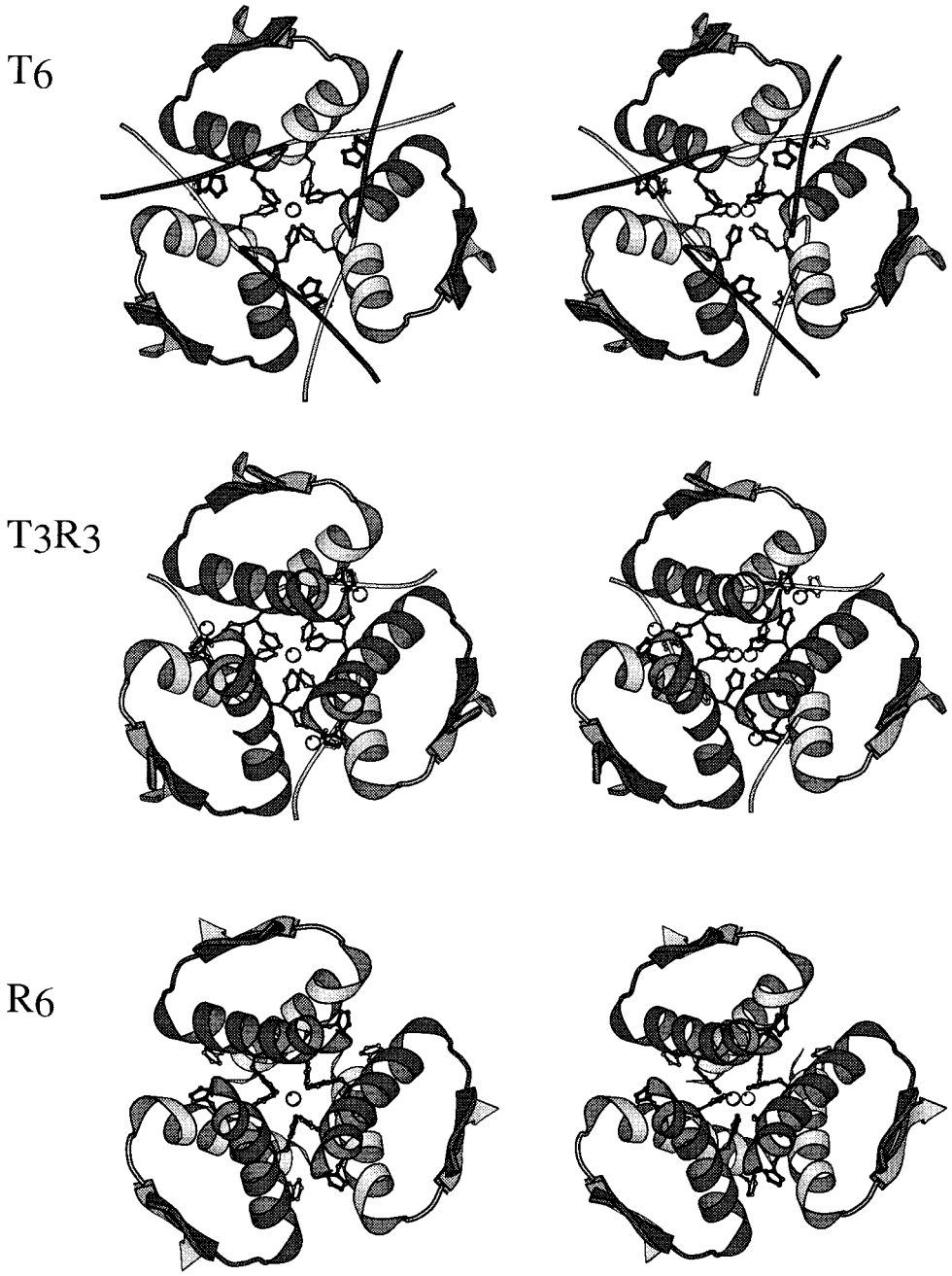

FIGURE 1: Stereographic representations of two-zinc pig insulin (T_6), four-zinc pig insulin (T_3R_3), and rhombohedral phenol insulin (R_6) hexamers viewed approximately parallel to the hexamer 3-fold axis. The insulin molecule consists of two polypeptide chains, an A chain of 21 amino acids and a B chain of 30 amino acids. These are covalently linked by interchain disulfide bridges between residues A7 and B7 and between A20 and B19 (*5*). The A chain is folded into two α-helices (A1−A8 and A13−A19) connected by a loop region (A9−A12). The B chain contains one central α-helix (B9−B19), with the N-terminal residues B1−B8 in either a helical or extended conformation, and the C-terminal residues B20−B30 extended. For clarity, only the B chains are shown, and in each dimer the two chains are shaded differently. The positions of the zinc ions (white spheres) and the side chains of residues B5 His and B10 His (ball-and-stick) are shown. Note that in the T_3R_3 hexamer residue B10 His can occupy one of two different conformations to coordinate to zinc ions both on and off the hexamer 3-fold axis. Hence, the off-axis zinc ion binding sites are only half occupied by metal ions, giving rise to an average of three zinc ions per hexamer (although for historical reasons this structure is termed four-zinc insulin). This figure was made by using MOLSCRIPT (*36*).

molecule 2 can be involved in additional off-axial zinc ion coordination at the dimer−dimer interfaces (*7, 9*). The R_6 hexamer is obtained only in the presence of phenolic ligands. These molecules bind inside the hexamer, making ring-stacking interactions with the side chains of B5 His at the dimer−dimer interfaces, thus stabilizing six B1−B8 α-helices (Figure 1) (*10, 11*). Both of the zinc ions at the center of the hexamer are relatively buried and have tetrahedral coordination owing to the close proximity of the B-chain N-terminal α-helices. As a result, zinc ion diffusion from the hexamer is slow, adding to the stability of the R_6 hexamer in solution (*12*). This phenomenon has a bearing on therapeutic insulin preparations, which generally contain both zinc ions and an antimicrobial phenolic additive.

It seemed possible that a tyrosine side chain at position B5 could substitute for phenol binding at the dimer−dimer interface, thereby promoting R_6 hexamer formation in the absence of a phenolic compound. The following studies have

Table 1: Crystallization Conditions for B5 Tyr Human Insulin

additive	ligand-free (T_3R_3)	with phenol (R_6)	with resorcinol (R_6)
insulin (mg)	10	10	10
0.02 M HCl (mL)	2.0	2.0	2.0
0.12 M zinc acetate (mL)		0.1	0.1
0.15 M zinc acetate (mL)	0.05		
0.2 M trisodium citrate (mL)	1.0	1.5	1.04
2.5% phenol (aqueous) (mL)		0.4	
5.0% resorcinol (aqueous) (mL)			0.4
acetone	1.0		
NaCl (mg)		120	120
pH	6.4−7.1	6.5−7.8	6.5−7.8

therefore been carried out to investigate the effect of the mutation B5 His → Tyr on hexamer assembly. A crystal structure of B5 Tyr insulin has been determined in the absence of a phenolic additive, and for comparison, structures have also been obtained in the presence of phenol and resorcinol (1,3-dihydroxybenzene). These ligands are capable of making many van der Waals contacts and hydrogen bonds at the dimer−dimer interfaces in the hexamer. Molecular modeling calculations were carried out to investigate the conformational preference of B5 Tyr side chain (molecule 1) in the ligand-free structure, which was seen to cause some conformational rearrangement at the hexamer surface.

MATERIALS AND METHODS

Crystallization. The recombinant B5 Tyr human insulin was prepared at the Novo Nordisk Research Laboratories (Denmark) and stored as dried powder at 4 °C prior to use in crystallization trials. The crystallization was carried out by the batch method, following the procedure for crystallizing wild-type R_6 and T_6 insulin hexamer (*13*, *14*). For each crystallization experiment, a protein solution was prepared by dissolving insulin in 0.02 M hydrochloric acid. Other crystallization components were then added in the order given in Table 1. The pH was adjusted with 0.5 M − 1.0 M HCl and NaOH until the solution obtained a slight turbidity, which dissolved on warming in a 50 °C water bath. In this way several supersaturated insulin samples were prepared at different pH values. Each sample was sealed in a glass tube with parafilm, placed in a prewarmed Dewar flask at 50 °C, and then left for 1 week, during which time crystals appeared.

Data Collection and Data Processing. Several crystals of the B5 Tyr mutant insulin grown in the absence of a phenolic ligand were tested, the diffraction generally being rather diffuse and weak at high resolution. Eventually, a suitable crystal was found and a 2.4 Å data set was collected at room temperature, using an RAXIS II image plate mounted on a Rigaku rotating-anode generator (λ = 1.542 Å). The data were processed with MOSFLM (*15*) and then scaled and merged by use of the CCP4 suite (*16*). A high overall temperature factor of 50 Å^2, as determined from a Wilson plot, was associated with the data set. It was therefore decided to "sharpen" the data by applying an artificial temperature factor of −20 Å^2 to the raw data. This had the effect of enhancing the contribution of the weak high-resolution data in the calculations of structure factors and electron density maps (*17*). Data statistics are given in Table 2.

Diffraction data for the B5 Tyr (phenol) insulin were collected on one crystal at room temperature with a Xentronics area detector (λ = 1.542 Å). The data were processed with the XDS package (*18*) and then scaled and merged by use of the CCP4 suite (*16*). X-ray diffraction data for the B5 Tyr (resorcinol) insulin were also collected on a single crystal at room temperature, this time using a Rigaku R-axis IIC image plate. The data set was processed with the program DENZO (*19*) and then scaled and merged by use of the CCP4 suite. Statistics for both data sets are listed in Table 2.

Refinement. The ligand-free B5 Tyr insulin structure was refined by using the coordinates for the isomorphous T_3R_3 four-zinc insulin structure as a starting model, which contains a dimer in the asymmetric unit (*7*). Prior to the refinement, most regions of the $3F_o - 2F_c$ map showed well-defined electron density. However, the areas containing the B5 Tyr side chains, B1 Phe of molecule 1, the B chain C-termini (B29 and B30), and residues A7−A10 in molecule 2 showed poor connectivity and therefore these parts of the protein structure were omitted from the model. In addition, the off-axial zinc ion was excluded owing to the lack of electron density in the $3F_o - 2F_c$ map and the negative density at its position in the $F_o - F_c$ map. Refinement proceeded with the least-squares minimization program PROLSQ (*16*) interspersed with structural remodeling by use of $3F_o - 2F_c$ and $F_o - F_c$ electron density maps, utilizing the program O (*20*). As the refinement continued, residues B5 Tyr (molecules 1 and 2), A10 Ile (molecule 2), and B29 Lys (molecules 1 and 2) could be modeled into the density maps and included in subsequent phasing calculations. Residue A8 Thr (molecule 2) was eventually assigned an occupancy of 0.5; its position (as determined from the $F_o - F_c$ map) was too close to the side chain of B5 Tyr of an adjacent hexamer for this residue to be fully occupied. In the final structure residues A7 Cys and A9 Ser (molecule 2) and B1 Phe of molecule 1 and B30 Thr (molecules 1 and 2) did not have any associated electron density and were therefore assigned occupancies of 0.0. Refinement parameters and statistics are summarized in Table 2.

For the crystal structures of B5 Tyr insulin with phenol and with resorcinol, the refinement procedures were similar. In each case the wild-type human insulin structure with phenol, containing a hexamer in the asymmetric unit, was used as the initial model (*10*). Before the refinement was begun, water molecules, counterions, phenol ligands, and residues B4−B6 (in the vicinity of the mutation) were removed, and atomic *B*-values were set to an average value of 20 Å^2 for main-chain atoms and 30 Å^2 for the side-chain atoms, respectively. Refinement was carried out with the program PROLSQ. Cycles of refinement were accompanied by examination of $2F_o - F_c$ and $F_o - F_c$ electron density maps. The maps were displayed on an Evans and Sutherland 10 graphics system, and the program FRODO (*21*) was used for the adjustment and modeling of protein atoms, counterions, ligands, and water molecules. The positions of the six mutated B5 Tyr side chains in the hexamer were clearly defined in the first electron density maps, and these residues were included in subsequent refinement cycles. Refinement proceeded until convergence. More refinement details are given in Table 2.

Molecular Modeling. Molecular modeling was used to investigate the observed conformational preferences of B5 Tyr (molecule 1, T state) in the T_3R_3 B5 Tyr insulin. Empirical potential energy calculations were performed with

Table 2: Data Processing and Refinement Statistics for the Crystal Structures of B5 Tyr Human Insulin

	ligand-free ($T_3R^f_3$)	with phenol (R_6)	with resorcinol (R_6)
space group	*R*3	$P2_1$	$P2_1$
cell dimensions (Å)	$a = 80.94$, $c = 37.62$	$a = 61.10$, $b = 62.08$, $c = 48.35$, $\beta = 109.9°$	$a = 60.81$, $b = 62.05$, $c = 47.65$, $\beta = 110.4°$
resolution limits (Å)	25.65−2.40	36.76−2.26	19.21−2.00
no. of unique reflections	3477	13 832	21 525
completeness of data[a] (%)	96.7 (92.1)	92.2 (95.5)	95.6 (87.6)
data redundancy[a]	2.5 (2.3)	1.8 (1.6)	2.5 (2.2)
R_{merge}[a,b] (on *I*)	4.6 (13.2)	4.6 (10.7)	5.8 (22.4)
reflections > 3σ[a] (%)	91.9 (75.1)	83.3 (69.5)	79.7 (45.1)
statistics for final structure			
rms Δ bond lengths[c] (Å)	0.021 (0.020)	0.011 (0.020)	0.011 (0.020)
rms Δ angle related distances[c] (Å)	0.054 (0.040)	0.037 (0.040)	0.036 (0.040)
$B_{average}$ for protein atoms[d] (Å^2)	20.1/22.0	31.2/35.9	35.0/39.7
final *R* factor[e] (all data) (%)	19.9	18.6	19.1

[a] Statistics for highest resolution shell are given in parentheses. [b] $R_{merge} = \Sigma|I - I_i|/\Sigma I$, where *I* is the mean intensity of the *N* reflections with intensities I_i. [c] Target restraints are given in parentheses. [d] Main-chain/side-chain values. [e] Crystallographic *R* factor $= \Sigma|F_o - F_c|/\Sigma F_o$, where F_o and F_c are the observed and calculated structure amplitudes, respectively.

the CHARMM program (*22*), utilizing the toph19/param19 potential (*23*). Crystallographic water molecules and zinc and chloride ions were retained. The zinc ion interaction parameters represented only nonbonded interactions (no explicit bond terms were included to maintain specific coordination) (*24*). The crystal structure of the B5 His → Tyr mutant was prepared by generating hydrogen positions necessary to fulfill the required atomic representation by using the HBUILD function of CHARMM (*25*). Conformational searches were performed on the side-chain dihedrals (χ_1 and χ_2) of B5 Tyr. One set of calculations considered the monomer in the dimer environment, representative of the molecule in solution. To reproduce the rhombohedral crystallographic environment, in which B5 is situated at a hexamer−hexamer interface, a double hexamer was constructed, bringing together three T-state B5 residues. Systematic searches of the χ_1 and χ_2 dihedrals were made at rotations of 10° and 45° for each of the respective environments described above. In the hexamer searches, the B5 dihedrals were changed synchronously, to reflect the crystallographic symmetry. At each point in the search the whole system was energy-minimized by a combination of steepest descent and Newton Raphson methods (*22*). In the initial stages of the minimization, the side-chain positions of the B5 residues were fixed and the rest of the atoms were allowed to relax around them. Subsequently, the system was extensively minimized without constraints until the rms[1] magnitude of the forces was lower than 10^{-5} kcal^{-1} mol^{-1} Å^{-1}. For computational efficiency, in the hexamer−hexamer system all atoms outside of 25 Å of the B5 residues were fixed. Previous work on localized conformational processes in proteins has shown that atoms more than 8−10 Å away have negligible contributions to the process (*26*). Moreover, analysis of structural changes in the dimer calculations suggest negligible movement of these distant atoms. Energy barriers for interconversion between selected minima were estimated by the conjugate peak refinement method implemented in CHARMM (*27*). The application of this methodology for localized conformational transitions in proteins has been outlined elsewhere (*26*).

[1] Abbreviation: rms, root-mean-square.

RESULTS

Structure of B5 Tyr (Human) T_3R_3 Insulin. Under conditions similar to those for T_6 insulin crystals (*6*), B5 Tyr insulin crystallizes as a T_3R_3 hexamer containing two zinc ions on the hexamer 3-fold axis. This structure is essentially identical to that of the native human insulin T_3R_3 hexamer crystallized with dilute phenol or chloride ions (*8, 32*). In B5 Tyr T_3R_3 insulin, however, the zinc ion at the center of the R_3 trimer is tetrahedrally coordinated to three B10 His side chains and a chloride ion, while in the T_3 trimer the complex arrangement of water molecules around the zinc ion represents a mixture of tetrahedral and octahedral coordination geometry (Figure 2). It has been suggested that small differences in pH or in the concentration of metal and halide ions in the crystallization conditions may result in different zinc coordination states (*8*). At the off-axial sites on the dimer−dimer interfaces, there is no additional zinc ion binding as seen in native T_3R_3 hexamer, since the B5 His → Tyr mutation eliminates the capacity to coordinate to zinc. Consequently, the side chain of B10 His occupies only one conformation in the direction of the hexamer 3-fold axis (cf. Figure 1). In many T_3R_3 hexamers, the B1−B8 α-helices of the R monomers are slightly unwound, or "frayed", at their N-termini, giving rise to the definition $T_3R^f_3$. The position of B1−B3 in the R monomer of B5 Tyr insulin suggests that this hexamer is of the form $T_3R^f_3$ (*8*).

In both molecules 1 and 2, the side chains of residue B5 Tyr adopt similar conformations to those of B5 His in the equivalent native T_3R_3 hexamer (Figures 3 and 4). The shape of the electron density for both of these side chains reflects a small degree of disorder, especially in the case of molecule 2 (R-state), for which the temperature factors for the main chain (25.6 Å^2) and side chain (31.2 Å^2) are a little higher than average (Table 2). This could be explained by the absence of any contact between the tyrosine side chain and the rest of the protein at the dimer−dimer interface. Furthermore, this area appears to contain only one water molecule, and even this does not hydrogen-bond to the hydroxyl group of the tyrosine. In molecule 1 (T-state), B5 Tyr is located on the surface of the hexamer. The tyrosine side chain, which is stabilized by van der Waals contacts with the side chain of residue A10 Ile of the same monomer, appears to be associated with perturbations of a nearby A7−

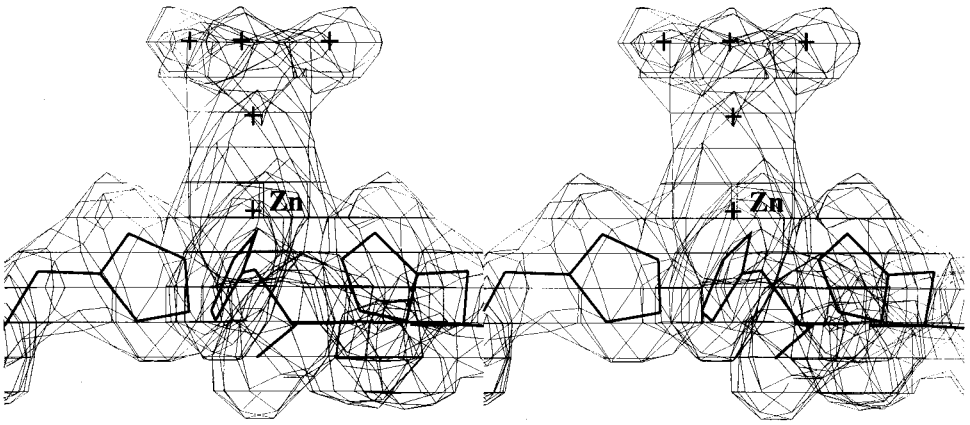

FIGURE 2: Stereoview parallel to the crystallographic 3-fold axis showing the zinc ion in the T_3 trimer of the B5 Tyr $T_3R^f_3$ insulin hexamer. The arrangement of water molecules above the zinc ion suggests that its coordination geometry is a mixture of octahedral and tetrahedral.

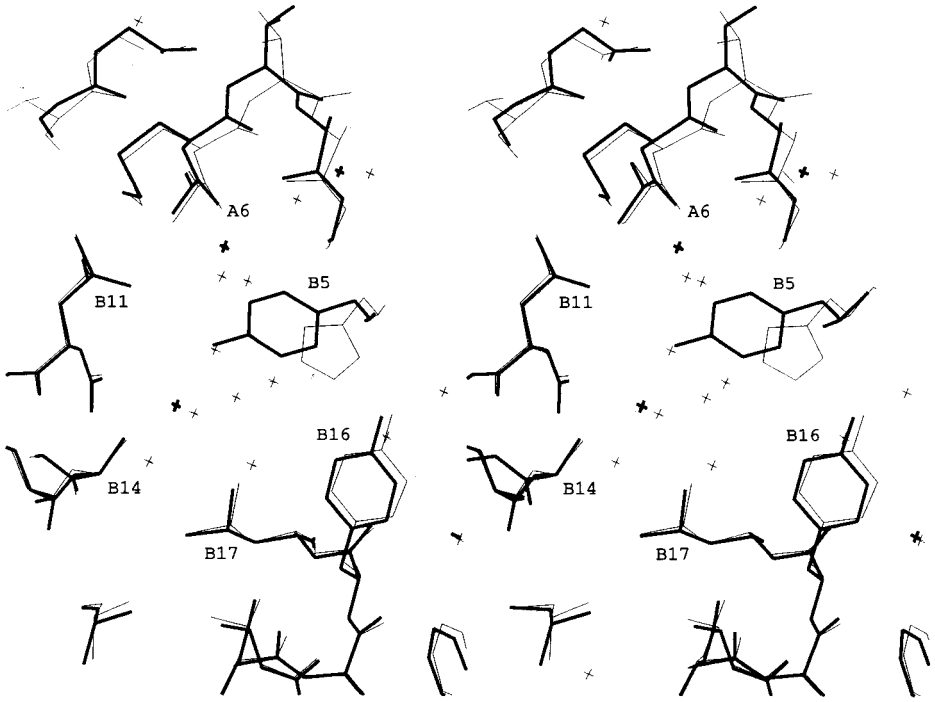

FIGURE 3: Stereoview of a superposition of the off-axis binding site in the R_3 trimer of $T_3R^f_3$ B5 Tyr insulin (heavy lines) and T_3R_3 human insulin (light lines) (*8*). Unlike four-zinc (pig) insulin as seen in Figure 1, this structure contains no zinc ions in the off-axis binding sites. The sites are almost identical except for the positions of the side chains of residues B5 His and B5 Tyr. The absence of water molecules in the B5 Tyr site reflects inherent disorder in the structure.

A11 loop (molecule 2) in an adjacent hexamer. Careful remodeling of this loop during refinement resulted in the loop residues being assigned the following occupancies: A7 Cys (0.0), A8 Thr (0.5), A9 Ser (0.0) and A10 Ile main chain (1.0). Residues A8 Ser and A10 Ile were displaced by 0.5−0.7 Å to avoid being too close to the B5 Tyr side chain (Figure 4), which in turn resulted in a similar displacement of residue A4 Glu (not shown). Given the quality of the electron density in this region, the detailed nature of these structural perturbations cannot be established unambiguously. However, the A7−A10 loop shows significant structural variations across the family of insulin structures (Tyrrell, Caves, and Dodson, unpublished results) and thus the poor density in this region may reflect dynamic and/or static disordering, in this case enhanced by the B5 Tyr side chain.

Molecular Modeling of B5 Tyr (Human) T_3R_3 Insulin. In the conformational searches, the resulting minimum energy structure has B5 Tyr side-chain dihedral angles close to those observed in the crystal structure (and closer than any other structure generated in the search, see Table 3); this was termed conformer I (Figure 5). The similarity of the lowest energy conformation in both the dimer and crystal-packing environments reflects the dominant nature of the intramolecular interactions of the B5 Tyr side chain in determining the overall conformation of this side chain. In investigating alternative conformations for this side chain, the search results were examined to determine the next lowest energy minima (the secondary minima) of significantly different χ_1 dihedral angles (i.e., transitioning at least 60°). For the dimer, this was found at $\chi_1 = 27°$, $\chi_2 = -103°$. This alternative conformation (conformer II), which is characterized by a change in χ_1 of approximately 100°, folds the side chain back against the surface of the dimer so that the hydroxyl group of B5 Tyr forms a hydrogen bond with the NE2 group of B4 Gln. In the crystal-packing environment, the next lowest minimum is found in an alternative conformation, $\chi_1 =$

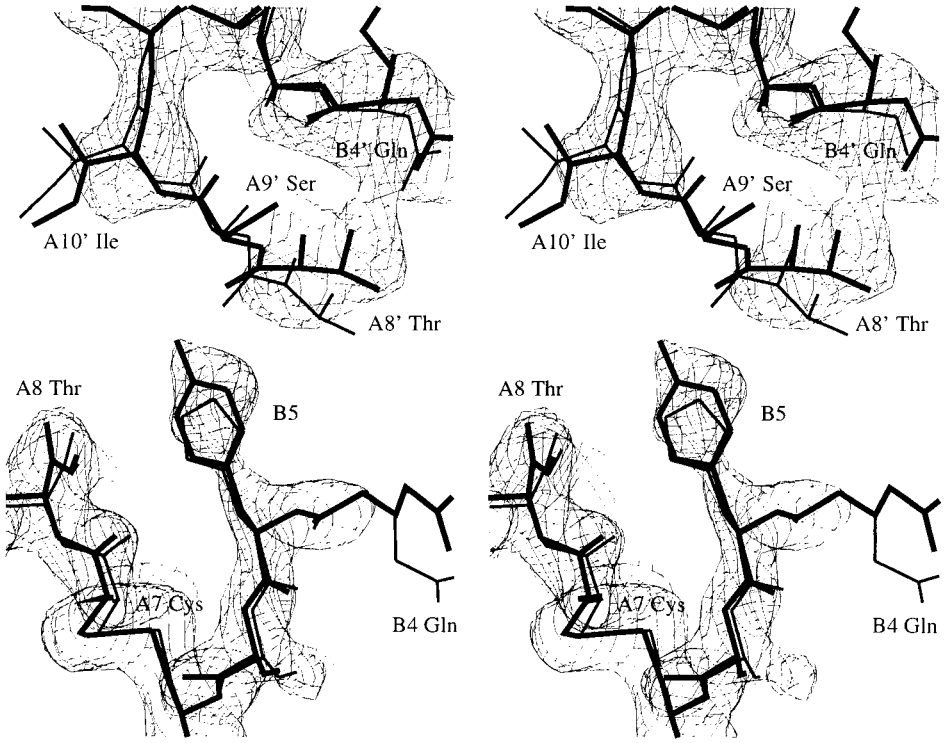

FIGURE 4: Stereoview of a comparison of $T_3R^f_3$ B5 Tyr insulin (heavy lines) and T_3R_3 human insulin (light lines) centered on residue B5 of molecule 1 (T state). Residue numbers are either unprimed or primed to show residues in adjacent hexamers. The electron density for the $T_3R^f_3$ B5 Tyr insulin structure, shown here by a $2F_o-F_c$ map, shows the structural rearrangement resulting from the B5 His → Tyr mutation. Residue A9′ Ser is disordered and residues A8 Thr and A10 Ile have moved significantly relative to the native structure.

Table 3: Side-Chain Dihedral Angles of B5 Tyr (Molecule 1) in the T_3R_3 Hexamer Crystal Structure and in Local Minima from the Conformational Searches in the Dimer and Hexamer Environments

environment	conformer	χ_1 (deg)	χ_2 (deg)	side-chain interactions
crystal structure		−67	−63	*a*
dimer	I	−88	−67	*b*
	II	27	−103	*c*
	III	−166	96	*d*
hexamers	I	−67	−34	*e*
	II	42	−97	*f*
	III	−170	95	*g*

[a] van der Waals contact to A10 Ile side chain of same monomer. Possible hydrogen bond (2.8 Å) between B5 Tyr OH and A8 Thr main-chain oxygen of adjacent hexamer. [b] van der Waals contact to residues of the same monomer, including the side chain of A10 Ile, main chain of A9 Ser, main chain of A8 Thr, and main chain of A7 Cys. [c] van der Waals contact to side chains of A4 Gln and A10 Ile of the same monomer. Possible hydrogen bond between B5 Tyr OH and B4 Gln NE2 (3.0 Å). [d] van der Waals contacts to the same monomer, including the main chain of A8 Thr, the side chain of A7 Cys, the main chain of A9 Ser, and the side chain of A10 Ile. [e] Possible hydrogen bond (2.5 Å) between B5 Tyr OH and A8 Thr main-chain oxygen of adjacent hexamer. Possible hydrogen bond between B5 Tyr OH and B4 Gln ND2 of same monomer. van der Waals contact to A10 Ile side chain and A9 Ser mainchain of same monomer. [f] van der Waals contact to main chain of A7 Cys and A8 Thr, and A3 Val side chain of adjacent hexamer. van der Waals contact to A7−B7 disulfide bridge of same dimer. [g] Hydrogen bond (2.5 Å) to B2 Val main chain of adjacent hexamer. van der Waals contact to A7 Cys and B7 Cys main chain of same monomer. van der Waals contact to side chain of B3 Gln of adjacent hexamer.

−170°, $\chi_2 = 95°$ (conformer III). Here the side chain makes an interhexamer hydrogen bond to the backbone carbonyl of B2 Val. The relative energies of these different conformations were computed for each of the closest corresponding local minima in both environments (Table 4). Compared to the dimer environment, the alternative conformations in the crystal-packing environment are relatively higher in energy with respect to the common ground-state conformer I (potential energy differences of 3.8 and 8.6 vs 37.4 and 37.5 kcal mol^{-1} for dimer and crystal-packing environments, respectively).

The picture that emerges is of the B5 side chain in the dimer environment having a well-defined primary conformation determined by local steric interactions. The secondary minima (conformers II and III) are very close in energy (difference of <8.6 kcal mol^{-1}) and can be interconverted at little cost (barriers of < 9.9 kcal mol^{-1}). By contrast, in the hexamer environment, the secondary minima are relatively higher in energy (differences of up to 37.5 kcal mol^{-1}) and have much larger barriers to interconversion (38 to 115 kcal mol^{-1}). Thus, the hexamer−hexamer interactions restrict the conformational space of the B5 Tyr side chain, resulting in one dominant conformation that projects toward the symmetry-related hexamer. In response, the other hexamer appears to undergo an extensive reorganization involving residues A7−A10 of one molecule; these residues required remodeling during crystallographic refinement (see earlier). Such conformational rearrangements were not addressed in the modeling studies.

Structure of B5 Tyr (Human) Insulin with Phenol. B5 Tyr (human) insulin with phenol was refined against data extending to 2.3 Å spacing using the refinement restraints listed in Table 2, which also gives statistics for the final set of coordinates. The structure is almost identical to that of monoclinic phenol insulin (*10*), having an average atomic displacement of 0.30 Å for all atoms of the hexamer that forms the asymmetric unit. The B5 Tyr phenol insulin

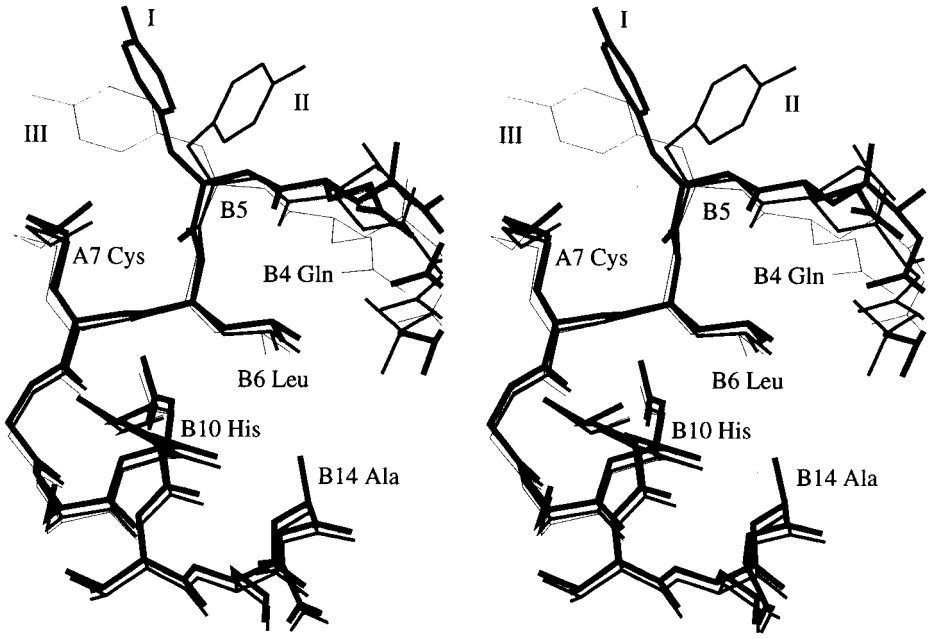

FIGURE 5: Stereoview of the structures corresponding to the three local minima for the side-chain conformation of B5 Tyr (molecule 1), resulting from the conformational search in the dimer environment. Conformer I (the lowest energy minimum, see Table 4) is very similar to the conformation observed in the crystal structure (cf. Figure 4) and is also the lowest energy minimum resulting from calculations of the hexamer−hexamer interface. The alternative conformations (II and III), although of low energy and easily accessible in the dimer, are significantly destabilized by the hexamer packing interactions (see Table 4).

Table 4: Relative Energetics and Barriers to Interconversion of Local Minima from the Conformational Searches in the Dimer and Hexamer Environments of B5 Tyr (Human) T_3R_3 Insulin[a,b]

	environment					
	dimer			hexamer		
conformer	I	II	III	I	II	III
I		3.8	8.6		37.5	37.4
II	7.9		4.8	38.0		−0.1
III	9.9	7.1		52.5	115.0	

[a] Energies are given in kilocalories per mole. [b] For each environment (dimer and hexamer) a matrix of interconformer relationships is presented for conformers I, II, and III (see Table 3). In each upper triangle the relative energetics of the different conformers are presented as potential energy differences of the respective local minima. In each lower triangle the barriers to interconversion of the different conformers are given as the potential energy differences of the local minimum to the transition state [computed by the conjugate peak refinement method of Fischer and Karplus (*27*); see text for details] for the transition from the columnwise conformer to the rowwise conformer.

hexamer contains two tetrahedrally coordinated zinc ions on the hexamer 3-fold axis, each with a chloride ion as the fourth ligand. At each of the three dimer−dimer interfaces there are two phenol ligands occupying similar binding sites. Each phenol forms van der Waals contact with the tyrosyl side chain of residue B5 Tyr and is also hydrogen-bonded to A6 O and A11 N of the adjacent dimer (Figure 6).

As the mutated residue is located inside the R_6 hexamer, it has no effect on crystal contacts. Furthermore, the positions of the phenol molecule and the mutated side chain, relative to those of the native structure, have hardly changed. The water structure does vary in each of the six crystallographically independent binding sites, giving rise to different hydrogen-bonding interactions at the dimer−dimer interfaces. In two of the sites, the B5 Tyr side chain hydrogen-bonds to the adjacent dimer through a bridging water molecule between B5 OH and A11 O (Figure 7A). In three other sites, the B5 Tyr hydroxyl groups hydrogen-bond to B10 O or B17 O of the adjacent monomer in the same dimer via a different water molecule (Figure 7B), while in the remaining site B5 tyrosyl hydroxyl group appears to make no hydrogen-bonding contact at all.

Structure of B5 Tyr (Human) Insulin with Resorcinol. B5 Tyr (human) insulin with resorcinol was refined to 2.0 Å spacing with the refinement parameters listed in Table 2. Table 2 also shows final refinement statistics, which indicate that the average temperature (*B*) factor for this structure is a little higher than that for the equivalent phenol-containing structure described above, despite higher resolution data and similar refinement strategies in the two cases. This may be explained by the observation that the resorcinol-containing structure has several more disordered side chains than the equivalent phenol structure. Generally, however, the B5 Tyr (resorcinol) insulin hexamer is very similar to the native insulin R6 (phenol) hexamer, showing an average atomic displacement of 0.28 Å for all protein atoms in the asymmetric unit. The B5 Tyr mutant insulin hexamer contains two tetrahedrally coordinated zinc ions on the 3-fold axis and two resorcinol molecules at each dimer−dimer interface. The hydrogen-bonding and van der Waals interactions made by each of the resorcinol molecules are the same as those made by resorcinol in the native structure, including a water bridge between A11 O and the second hydroxyl group of resorcinol.

As in the phenol complex, where the hydrogen-bonding contacts of the B5 tyrosine OH group varies in the different subunits, the six resorcinol binding sites are not completely identical. In three of the binding sites, the B5 Tyr OH group forms a hydrogen bond to a water molecule associated with resorcinol, thus forming an extra contact between the dimers (Figure 8A). However, in the fourth binding site the B5 Tyr OH group hydrogen-bonds directly to resorcinol (Figure 8B).

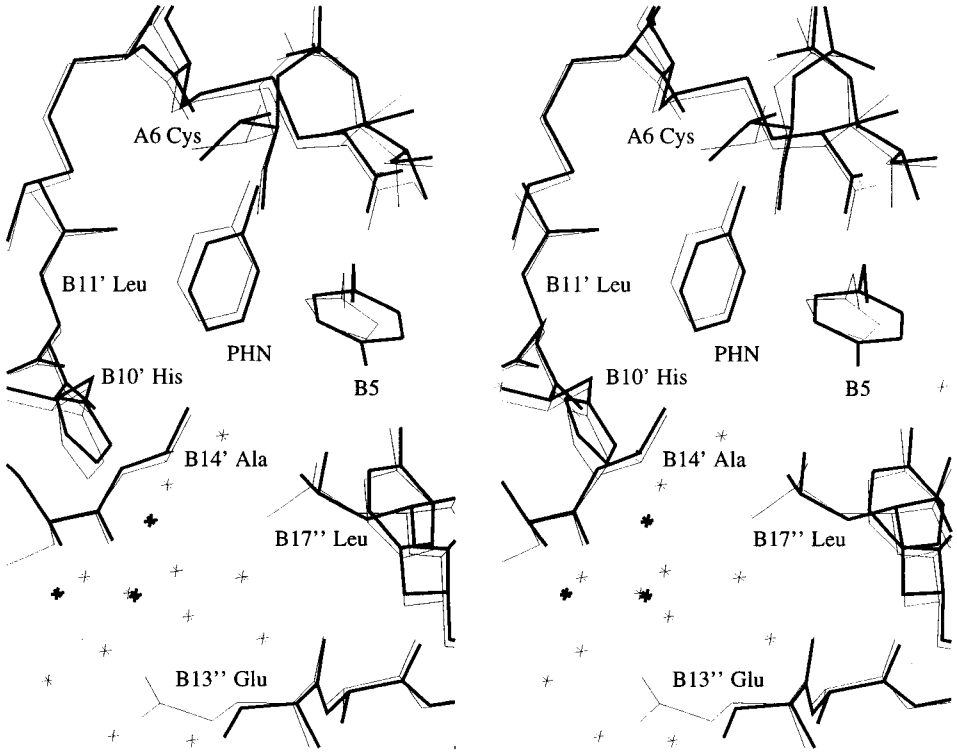

FIGURE 6: Stereoview showing a superposition of the phenol binding sites in R_6 B5 Tyr insulin hexamer (heavy lines) and native R_6 insulin (light lines) (*10*). The mutation has very little effect on the positions of the phenol molecule of the surrounding side chains.

The last two B5 Tyr OH hydrogen bonds to B17 O of the adjacent monomer in the same dimer are via a different water molecule.

DISCUSSION

The B5 His → Tyr mutation is one in a series of mutagenesis studies that have been carried out to investigate the aggregation properties of insulin. These have included selected point mutations at the monomer−monomer interface such as $B16^{His}$ (*28*), $B28^{Asp}$ (*1, 2, 29*), and $B28^{Lys}B29^{Pro}$ (*3*), which give rise to insulins that are predominantly monomeric at physiological concentrations. Also, mutations have been made that affect zinc ion coordination, for example, B10 His → Asp (*1, 30)*. These studies have applications for insulin therapy since the rate of action of injected insulin can, to some extent, be controlled by the rate of dissociation of the hexamers (*31*). In native insulin, residue B5 His does not have a clearly defined role. It is neither critical for receptor binding nor, it appears, functional in dimer or hexamer formation. Nevertheless, in the hexamer B5 His has a fascinating ability to coordinate zinc ions and interact favorably with phenolic molecules (*7, 10, 11, 32*). Furthermore, sequence alignments of insulins from diverse physiological sources reveal that when B10 His is present it is almost always accompanied by B5 His, indicating that the latter may have a role in hexamer assembly.

In the present study, different crystallization conditions have been used to explore the effect of the B5 His → Tyr mutation in hexameric insulin. When phenol or resorcinol is present in the crystallization medium, R_6 hexamers are obtained. In these cases, the effect of the mutation is almost neutral since B5 Tyr, despite its different size and hydrogen-bonding character, adopts an equivalent position to B5 His at the dimer−dimer interface, interacting with phenolic ligands in an analogous fashion. Compared with the native structure, there are only small differences at the dimer−dimer interfaces where the B5 tyrosine OH group and the phenolic ligand introduce a few extra hydrogen bonds through ordered water molecules. In the absence of phenolic ligand, B5 Tyr insulin crystallizes as a T_3R_3 hexamer in which B5 Tyr (molecule 2) is situated at the dimer−dimer interface of the R_3 trimer. The tyrosine side chain, however, does not make any interdimer contacts analagous to phenol, showing that it does not serve to stabilize the R-state molecules in the same way. To examine the origins of the observed T_3R_3 conformation, a simple modeling study was carried out in which all of the B5 His side chains in the native T_6 insulin hexamer were substituted by tyrosine residues. With the bulkier side chain, the ring-stacking interaction characteristic of B5 His was not possible, as one of the tyrosine side chains would have to undergo a significant conformational rearrangement to avoid a steric clash with the adjacent hexamer. Therefore, it is quite feasible that the B5 Tyr insulin hexamer adopts the T_3R_3 state in order to remove B5 Tyr (molecule 2) from the surface of the hexamer. This transition, which is low energy in the native structure [$\sim$2 kcal mol^{-1} (*33*)], is likely to be easier in the case of B5 Tyr insulin since intramolecular hydrogen bonds made by the side chain of B5 His that stabilize the T state in the native insulin hexamer are no longer present (*6*).

In the T_3 trimer of the T_3R_3 B5 Tyr insulin hexamer, B5 Tyr (molecule 1) is located on the surface of the hexamer where it adopts a similar conformation to the native B5 His side chain (Figure 4). The position of the larger tyrosine side chain is, however, associated with significant disorder in the A7−A10 loop of molecule 2 in the adjacent hexamer. On steric grounds, such structural perturbations could potentially be avoided by a rotation of approximately 180° around χ_1

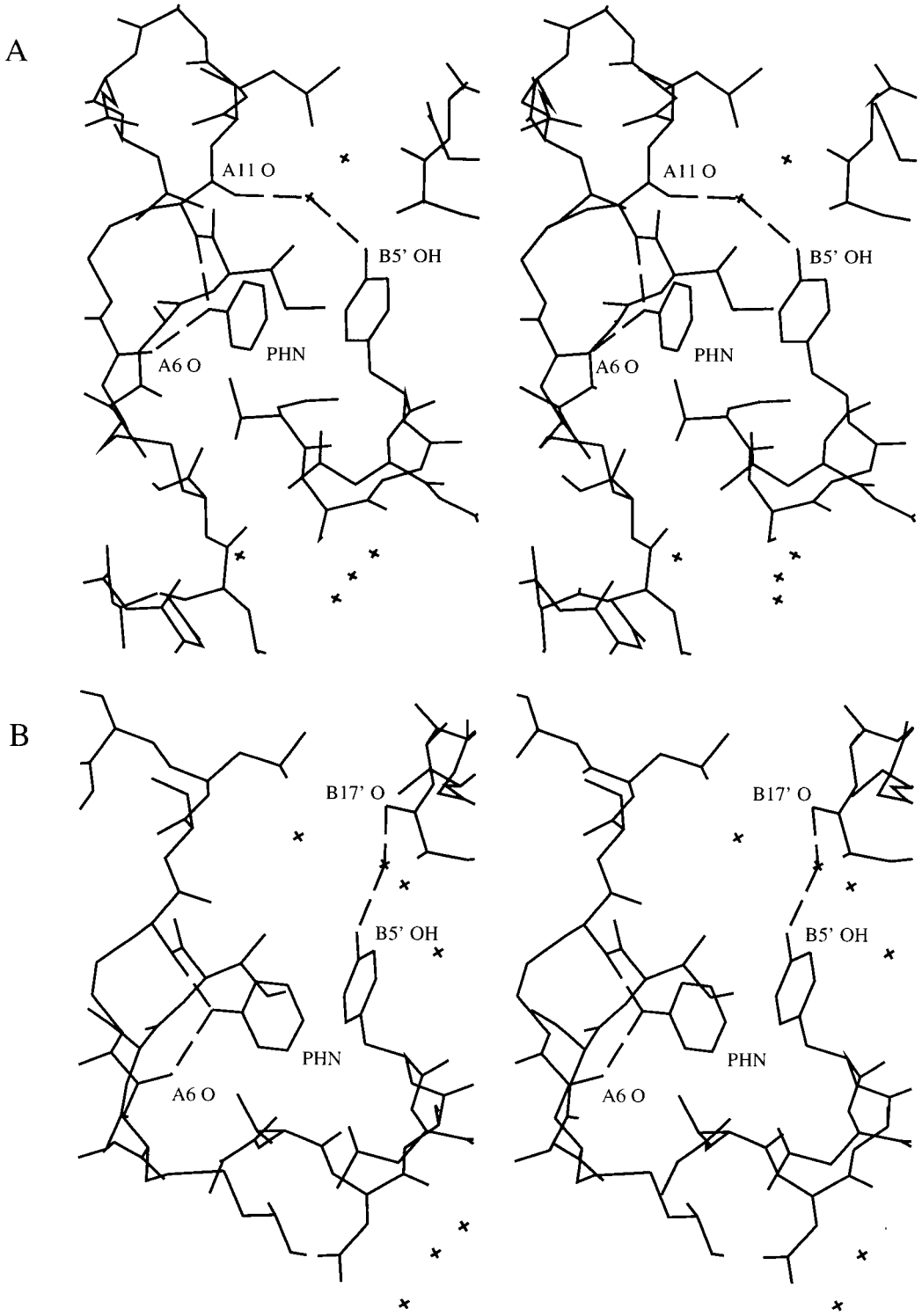

FIGURE 7: Stereoviews showing the hydrogen-bonding pattern for the phenol molecule (PHN) and the B5 Tyr side chain as it appears in two different sites in the R_6 B5 Tyr (phenol) insulin hexamer. Residues of different dimers are labeled as unprimed or primed. (A) The tyrosine side chain makes a dimer−dimer contact to A11 O of the adjacent dimer via a bridging water molecule. (B) The B5 Tyr side chain makes an intradimer hydrogen bond to either B16 O or B17 O via a bridging water molecule.

of B5 Tyr. To investigate this possibility, energy minimization studies were carried out to calculate the energies of alternative conformational transitions for the B5 Tyr side chain (molecule 1). The results for the isolated dimer reveal several possible low-energy conformations. Interconversions between these different minima are quite feasible at room temperature, since the enthalpic energy barriers that separate them are low. Moreover, the free energy barriers are likely to be further lowered by the higher entropies of the transition states with respect to the ground states. (The structures of the transition states are characterized by fewer contacts between the tyrosine side chain and the protein when compared to the ground state; see for example ref *26*.) In the hexamer−hexamer model, the tyrosine side chain lies at the interface, and although the lowest energy minimum (ground state) is the same as the dimer (conformer I), the

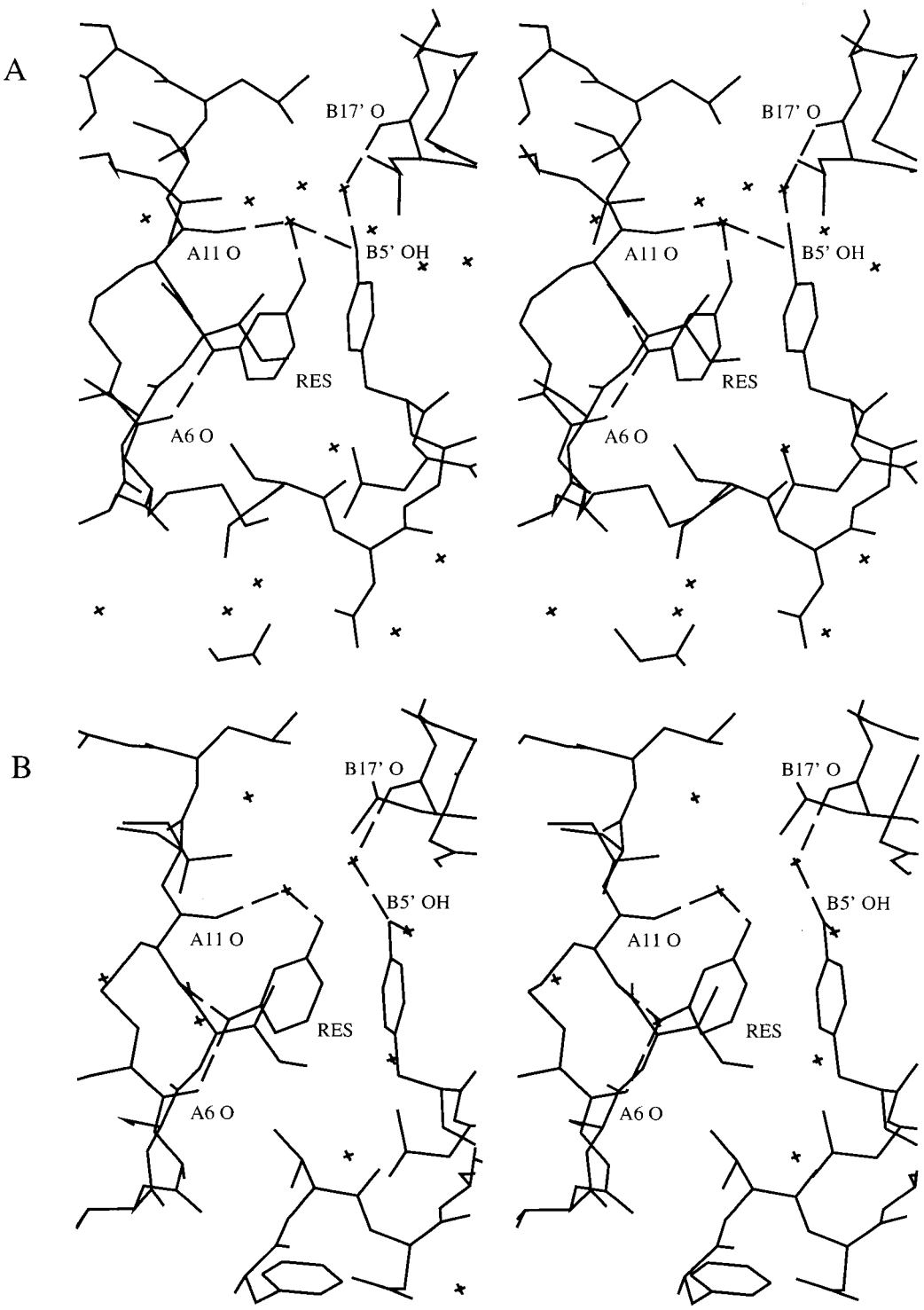

FIGURE 8: Stereoviews showing the hydrogen-bonding pattern of the resorcinol molecule (RES) and the B5 Tyr side chain as it appears in two different sites in the R_6 B5 Tyr (resorcinol) insulin hexamer. Residues of different dimers are labeled as unprimed or primed. (A) The tyrosine side chain and the resorcinol molecule make dimer−dimer contact via a bridging water molecule. (B) The B5 Tyr side chain makes an intradimer hydrogen bond to B17 O.

secondary minima are relatively higher in energy and the additional steric interactions make the barriers to interconversion very high. Thus, out of the three possible minima considered in the dimer only the observed ground-state conformer (conformer I) is selected upon assembling into the hexamers in the crystal structure. Hence, there is a local steric preference for keeping the tyrosine side chain in conformer I even though this appears to result in perturbations in a loop of the adjacent hexamer.

To conclude, our results suggest that in the rhombohedral insulin crystals, the B5 His → Tyr mutation destabilizes the T-state (through loss of relevant hydrogen bonds and through steric clashes) rather than stabilizing the R-state as anticipated. A complete transition to the R_6 state is unlikely to occur in the absence of a phenolic ligand since the energy barrier for the $T_3R_3 \rightarrow R_6$ transition is significantly higher than that for the $T_6 \rightarrow T_3R_3$ transformation (*33*). The structural disorder observed for residues A7−A10 (molecule

2) of the B5 Tyr T_3R_3 hexamer appears to be the result of a stiff local conformational preference at B5 Tyr (molecule 1). It is interesting that another packing arrangement was not selected so as to avoid B5 Tyr being involved in crystal contacts altogether. Regarding the physiological role of residue B5 His, one possibility is that it promotes the formation of rhombohedral hexamer packing in the insulin storage vesicles in the β-cell, as it does in the crystals. This would aid efficient packing of insulin in the vesicles, since rhombohedral insulin crystals have a lower solvent content (35−40%) than other crystalline forms of insulin [e.g., in monoclinic (phenol) insulin it is 50%]. Furthermore, electron micrographs of rat β granules and those of some other species show evidence of rhombohedral packing formations (*34*). Finally, although the B5 His → Tyr mutation did not stabilize the R-state in the way anticipated, its observed tendency to crystallize in the T_3R_3 state could give it an application as a slow-acting insulin, since native T_3R_3 insulin crystals have already been used for this purpose (*35*).

ACKNOWLEDGMENT

We are very grateful for the gift of B5 Tyr insulin from Novo Nordisk A/S, Denmark. We thank Steve Gamblin and Kim Henrick for advice during data processing, Roland Stote and Anthony Wilkinson for helpful discussions, and Stefan Fischer for making available developmental software.

REFERENCES

1. Brange, J., Ribel, U., Hansen, J. F., Dodson, G., Hansen, M. T., Havelund, S., Melberg, S. G., Norris, F., Norris, K., Snel, L., Sørensen, A. R., and Voigt, H. O. (1988) *Nature 333*, 679−682.
2. Brems, D. N., Alter, L. A., Beckage, M. J., Chance, R. E., DiMarchi, R. D., Green, L. K., Long, H. B., Pekar, A. H., Shields, J. E., and Frank, B. H. (1992) *Protein Eng. 5*, 527−533.
3. Ciszak, E., Beals, J. M., Frank, B. H., Baker, J. C., Carter, N. D., and Smith, G. D. (1995) *Structure 3*, 615−622.
4. Markussen, J., Havelund, S., Kurtzhals, P., Andersen, A. S., Halstrøm, J., Hasselager, E., Larsen, U. D., Ribel, U., Schäffer, L., Vad, K., and Jonassen, I. (1996) *Diabetologia 39*, 281−288.
5. Adams, M. J., Blundell, T. L., Dodson, E. J., Dodson, G. G., Vijayan, M., Baker, E. N., Harding, M. M., Hodgkin, D. C., Rimmer, B., and Sheat, S. (1969) *Nature 224*, 491−495.
6. Baker, E. N., Blundell, T. L., Cutfield, J. F., Cutfield, S. M., Dodson, E. J., Dodson, G. G., Crowfoot Hodgkin, D. M., Hubbard, R. E., Issacs, N. W., Reynolds, C. D., Sakabe, K., Sakabe, N., and Vijayan, N. M. (1988) *Philos. Trans. R. Soc. London 319*, 369−456.
7. Bentley, G., Dodson, E., Dodson, G., Hodgkin, D., and Mercola, D. (1976) *Nature 261*, 166−168.
8. Ciszak, E., and Smith, G. D. (1994) *Biochemistry 33*, 1512−1517.
9. Smith, G. D., Swenson, D. C., Dodson, E. J., Dodson, G. G., and Reynolds, C. D. (1984) *Proc. Natl. Acad. Sci. 81*, 7093−7097.
10. Derewenda, U., Derewenda, Z., Dodson, E. J., Dodson, G. G., Reynolds, C. D., Smith, G. D., Sparks, C., and Swenson, D. (1989) *Nature 338*, 594−597.
11. Smith, G. D., and Dodson, G. G. (1992) *Biopolymers 32*, 441−445.
12. Kaarsholm, N. C., Ko, H. C., and Dunn, M. F. (1989) *Biochemistry 28*, 4427−4435.
13. Schlichtkrull, J. (1958) *Insulin Crystals*, Ph.D. Thesis, University of Copenhagen, Denmark.
14. Harding, M. M., Hodgkin, D. C., Kennedy, A. F., O'Connor, A., and Weitzmann, P. D. J. (1966) *J. Mol. Biol. 16*, 212−226.
15. Leslie, A. G. W., Brick, P., and Wonacott, A. J. (1986) *CCP4 Newsl. 18*, 33−39.
16. Collaborative Computational Project, Number 4 (1994) *Acta Crystallogr. D50*, 760−763.
17. Gamblin, S. J., Rodgers, D. W., and Stehle, T. (1996) *Proceedings of the CCP4 Study Weekend*, pp 163−169, Daresbury Laboratory, Warrington, U.K.
18. Kabsch, W. (1988) *J. Appl. Crystallogr. 21*, 916−924.
19. Otwinowski, Z. (1993) in *Proceedings of the CCP4 Study Weekend*, pp 56−62, Daresbury Laboratory, Warrington, U.K.
20. Jones, T. A., Zou, J. Y., Cowan, S. W., and Kjeldgaard, M. (1991) *Acta Crystallogr. A47*, 110−119.
21. Jones, T. A. (1985) *Methods Enzymol. 115*, 157−171.
22. Brooks, B. R., Bruccoleri, R. E., Olafson, B. D., States, D. J., Swaminathan, S., and Karplus, M. (1983) *J. Comput. Chem. 4*, 187−217.
23. Neria, E., Fischer, S., and Karplus, M. (1996) *J. Chem. Phys. 105*, 1902−1921.
24. Stote, R. H., and Karplus, M. (1995) *Proteins: Struct., Funct., Genet. 23*, 12−31.
25. Brunger A. P., and Karplus, M. (1988) *Proteins: Struct., Funct., Genet. 4*, 148−156.
26. Verma, C. S., Fischer, S., Caves, L. S. D., Roberts, G. C. K., and Hubbard, R. E. (1996) *J. Phys. Chem. 100*, 2510−2518.
27. Fischer, S., and Karplus, M. (1992) *Chem. Phys. Lett. 194*, 252−261.
28. Ludvigsen, S., Roy, M., Thøgersen, H., and Kaarsholm, N. C. (1994) *Biochemistry 33*, 7998−8006.
29. Whittingham, J. L., Edwards, D. J., Antson, A. A., Clarkson, J., and Dodson, G. G. (1998) *Biochemistry 37*, 11516−11523.
30. Dodson, E. J., Dodson, G. G., Hubbard, R. E., Moody, P. C. E., Turkenburg, J., Whittingham, J., Xiao, B., Brange, J., Kaarsholm, N., and Thogersen, H. (1993) *Philos. Trans. R. Soc. London A 345*, 153−164.
31. Brange, J. (1997) *Diabetologia 40*, S48−S53.
32. Whittingham, J. L., Chaudhuri, S., Dodson, E. J., Moody, P. C. E., and Dodson, G. G. (1995) *Biochemistry 34*, 15553−15563.
33. Jacoby, E., Krüger, P., Karatas, Y., and Wollmer, A. (1993) *Biol. Chem. Hoppe-Seyler 374*, 877−885.
34. Greider, M. H., Howell, S. L., and Lacy, P. E. (1969) *J. Cell Biol. 41*, 162.
35. Brange, J. (1987) *Galenics of insulin. The physicochemical and pharmaceutical aspects of insulin and insulin preparations*, pp 26−27, Springer-Verlag, Berlin and Heidelberg, Germany.
36. Kraulis, P. J. (1991) *J. Appl. Crystallogr. 24*, 946−950.

BI990700K